JOURNAL OF SOLID STATE CHEMISTRY 118, 219–226 (1995)

Preparation, Properties, and Crystal Structures of Ti_3Zn_{22} and $TiZn_{16}$

Xue-an Chen,[1] Wolfgang Jeitschko,[2] Martin E. Danebrock, Christoph B. H. Evers, and Klaus Wagner

Anorganisch-Chemisches Institut, Universität Münster Wilhelm-Klemm-Strasse 8, D-48149 Münster, Germany

Received December 15, 1994; accepted February 15, 1995

Single crystals of Ti_3Zn_{22} and $TiZn_{16}$ were isolated from slowly cooled zinc-rich samples by dissolving their matrices in hydrochloric acid, which attacks the titanium-containing crystals at a lower rate. Both compounds are Pauli paramagnetic and show metallic conductivity. Their crystal structures were determined from single-crystal X-ray data. Ti_3Zn_{22} is of a new structure type with tetragonal symmetry: $P4_2/mbc$, $a = 1152.3(1)$, $c = 1145.6(2)$ pm, $Z = 4$, $R = 0.020$ for 920 structure factors and 64 variable parameters. The titanium atoms occupy two different sites with the coordination numbers 15 and 16, respectively, and one titanium position shows mixed occupancy, which results in the exact composition $Ti_{2.841(8)}Zn_{22.159(8)}$. The seven different zinc atoms have between 11 and 14 near neighbors. The previously reported structure of $TiZn_{16}$ is confirmed: $Cmcm$, $a = 769.9(3)$, $b = 1141.4(4)$, $c = 1180.0(3)$ pm, $Z = 4$, $R = 0.022$ for 787 structure factors and 50 variables. Both structures can be described as packings of different atomic layers. These layers are densely populated by zinc atoms or less densely populated by both titanium and zinc atoms. Both structures contain relatively large voids and it is suggested that these voids are filled with nonbonding electrons of the zinc atoms.

INTRODUCTION

The binary system titanium–zinc has been investigated in the past by Heine and Zwicker (1), Rossteutscher and Schubert (2), and Rennhack (3). The compounds proposed as equilibrium phases include Ti_2Zn with $MoSi_2$-type structure (2), TiZn with CsCl structure (1), $TiZn_2$ with the Laves phase structure $MgZn_2$ (4), and the Cu_3Au-type phase $TiZn_3$ (4). The crystal structures of the low-melting compounds at the zinc-rich side of that binary system are less well established, even though this part of the phase diagram has been studied by several investigators, because small additions of titanium to zinc act as grain refiners, which promote creep resistance in rolled alloys (5; references therein). There is a eutectic at 419°C (3) between zinc and a compound for which the crystal structure determination resulted in the composition $TiZn_{16}$ (6). This compound was formerly designated with the approximate composition "$TiZn_{15}$" (1, 3). According to the phase diagram as given by Rennhack (3), there occur at least two more compounds between $TiZn_3$ and $TiZn_{16}$, which are formed by a cascade of peritectic reactions. Only one of these (with the tentative composition "$TiZn_5$") is indicated in the phase diagram of Heine and Zwicker (1). However, the powder diagram reported by these authors for "$TiZn_5$" does not agree with the powder diagram of Ti_3Zn_{22} characterized in the present investigation. We also confirm the crystal structure of $TiZn_{16}$ and report electrical conductivity and magnetic properties of Ti_3Zn_{22} and $TiZn_{16}$. The structure determination of Ti_3Zn_{22} resulted in a mixed occupancy for one titanium position. Thus, the exact composition is $Ti_{2.841(8)}Zn_{22.159(8)}$; however, for simplicity we retained the ideal formula for most purposes.

SAMPLE PREPARATION AND LATTICE CONSTANTS

Starting materials were titanium powder and granules of zinc, both with stated purities greater than 99.9%. For the preparation of Ti_3Zn_{22}, an alloy containing 95 at.% zinc was sealed in an evacuated silica tube. The sample was equilibrated for two days at 850°C, slowly cooled (5°C/h) to 500°C, and quenched in air. After this treatment the sample consisted of Ti_3Zn_{22} crystals, which were embedded in a zinc-rich matrix. The crystals had the form of prisms with dimensions of up to $0.3 \times 0.3 \times 1.0$ mm^3. They were separated from the matrix by diluted hydrochloric acid, which attacks the matrix faster than the crystals of Ti_3Zn_{22}. The crystals of $TiZn_{16}$ were prepared in the same way, except that the starting composition contained 97 at.% zinc and the slow cooling was extended to 455°C. After the treatment in hydrochloric acid $TiZn_{16}$ crystals of up to a size of $0.3 \times 0.3 \times 4.0$ mm^3 were observed.

The well-crystallized samples of both compounds are grey with metallic luster. They are stable in air over long periods of time but are slowly attacked by diluted hydrochloric acid. Energy-dispersive X-ray analyses in a scan-

[1] Permanent address: Institute of Chemistry, Academica Sinica, Beijing 100080, People's Republic of China.

[2] To whom correspondence should be addressed.

0022-4596/95 $12.00

TABLE 1
Some Data and Results of the Structure Determinations of $Ti_{2.841(8)}Zn_{22.159(8)}$ and $TiZn_{16}$

Structure type	Ti_3Zn_{22}	$TiZn_{16}$
Crystal dimensions (μm^3)	120 × 100 × 50	80 × 50 × 30
Space group	$P4_2/mbc$ (No. 135)	$Cmcm$ (No. 63)
Lattice constants[a]		
	From powder data	
a (pm)	[1152.6(2)]	769.9(3)
b (pm)	—	1141.4(4)
c (pm)	[1143.2(9)]	1180.0(3)
V (nm^3)	[1.5187]	1.0369
	From single-crystal data	
a (pm)	1152.3(1)	[769.8(1)]
b (pm)	—	[1141.4(2)]
c (pm)	1145.6(2)	[1177.2(1)]
V (nm^3)	1.5211	[1.0343]
Formula units/cell	$Z = 4$	$Z = 4$
Formula mass	1584.8	1094.0
Calculated density (g/cm^3)	$\rho = 6.92$	$\rho = 7.01$
$\theta/2\theta$ scans up to	$2\theta = 73°$	$2\theta = 80°$
Range in hkl	±19, 0–19, 0–19	−13–2, ±20, ±21
Total number of reflections	7972	7602
Unique reflections	2197	1809
Inner residual	$R_i = 0.090$	$R_i = 0.083$
Reflections with $I > 3\sigma(I)$	920	787
Highest/lowest transmission	2.05	1.18
Number of variables	64	50
Conventional residual	$R = 0.020$	$R = 0.022$
Weighted residual	$R_w = 0.020$	$R_w = 0.026$

Note. Standard deviations in the positions of the least significant digits are given in parentheses throughout the paper.

[a] We considered the lattice constants of Ti_3Zn_{22} obtained from the single-crystal diffractometer data to be more accurate; for $TiZn_{16}$ we judged those from the powder data as more reliable (see text).

ning electron microscope did not reveal any impurity elements heavier than sodium.

The powders of Ti_3Zn_{22} and $TiZn_{16}$ used for the determination of the lattice constants were obtained by annealing cold-pressed pellets of the elemental components with the ideal compositions at 320°C for two weeks. The Guinier powder patterns were standardized with α-quartz (a = 491.30 pm, c = 540.46 pm). In general, the lattice constants obtained from powder data are more reliable, because those from single crystals are affected by systematic errors due to absorption. However, in the case of Ti_3Zn_{22} the constants obtained from the powder data were judged to be of lower accuracy than those obtained from the four-circle diffractometer, because the a and c axes of that tetragonal structure are of very similar lengths and therefore most reflections overlap. Thus, only 13 unambiguously assigned reflections were used for the powder data refinement. Lattice constants for $TiZn_{16}$ obtained from the powder data are listed in Table 1 together with other data of the structure determinations.

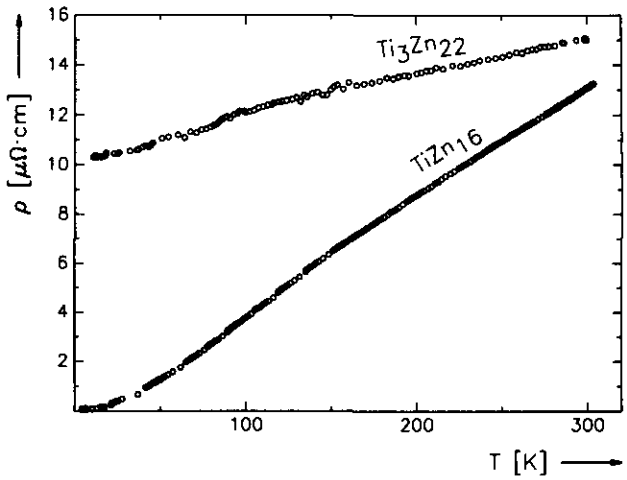

FIG. 1. Temperature dependence of the specific resistivity of Ti_3Zn_{22} and $TiZn_{16}$.

PHYSICAL PROPERTIES

The electrical conductivities of both compounds were determined with a four-probe technique. The electrical contacts were made by fine copper wires, which were attached to the crystals with well conducting silver pastes. A constant alternating current was maintained through the whole length of the sample and the potential difference was measured between the other two contacts. Figure 1 shows the temperature dependence of the specific electrical resistivities for Ti_3Zn_{22} and $TiZn_{16}$. Ti_3Zn_{22} is low-melting and partly melted upon annealing the silver epoxy so that the residual resistivity is large at low temperature. The resistivity increases with temperature, indicating metallic behavior expected for compounds with such compositions. Specific resistivities of about 15 $\mu\Omega \cdot$ cm for

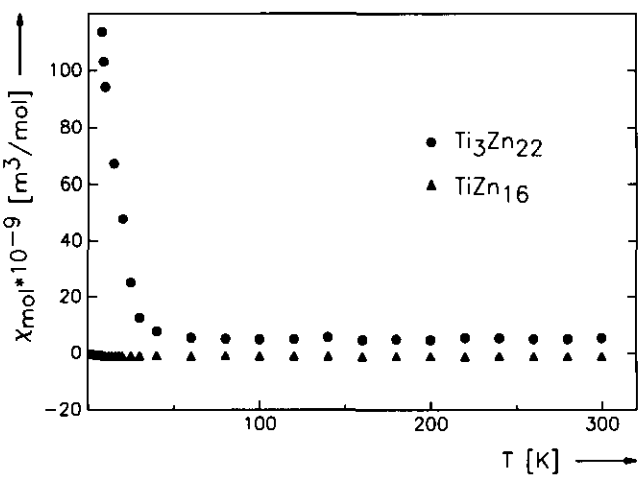

FIG. 2. Magnetic susceptibility of Ti_3Zn_{22} and $TiZn_{16}$ as a function of temperature.

Ti_3Zn_{22} and of about 13 $\mu\Omega \cdot$ cm for $TiZn_{16}$ were obtained at room temperature; they are between those of zinc (ρ = 5.9 $\mu\Omega \cdot$ cm) and titanium (ρ = 42 $\mu\Omega \cdot$ cm), which indicates that both Ti_3Zn_{22} and $TiZn_{16}$ are good metallic conductors.

The magnetic susceptibilities of selected Ti_3Zn_{22} and $TiZn_{16}$ single crystals were measured with a SQUID magnetometer at temperatures between 2 and 300 K at magnetic flux densities of 3 T. The magnetic susceptibility is approximately constant with an average of 5.11×10^{-9} m^3/mole between 50 and 300 K for Ti_3Zn_{22}. $TiZn_{16}$ shows temperature-independent diamagnetism with a smaller susceptibility of $\chi = -0.91(\pm 0.80) \times 10^{-9}$ m^3/mole (Fig. 2). Both values compare well with the molar susceptibilities of the metals titanium ($\chi = 1.92 \times 10^{-9}$ m^3/mole) and zinc ($\chi = -1.16 \times 10^{-10}$ m^3/mole). Irregardless of the negative susceptibilities of $TiZn_{16}$ and Zn, both binary compounds and elemental titanium and zinc may be considered to be Pauli paramagnetic after the correction for the core diamagnetism. The susceptibility increase of Ti_3Zn_{22} below 50 K is probably due to a small amount of an unknown paramagnetic impurity or to paramagnetic surface states.

STRUCTURE DETERMINATIONS

Single crystals of Ti_3Zn_{22} and $TiZn_{16}$ were investigated in Buerger precession cameras to establish their symmetry and suitability for the intensity data collections. Ti_3Zn_{22} showed a primitive tetragonal cell with the Laue symmetry $4/mmm$. The systematic extinctions (reflections $0kl$ were observed only with $k = 2n$ and hhl with $l = 2n$) led to the space groups $P4_2bc$ and $P4_2/mbc$, of which the higher symmetry group $P4_2/mbc$ was found to be correct during the structure refinement. $TiZn_{16}$ showed the same symmetry $Cmcm$ as already reported by Saillard *et al.* (6).

The X-ray diffraction data for both compounds were collected at room temperature on an automated four-circle diffractometer with graphite-monochromated Mo$K\alpha$ radiation and a scintillation counter with pulse-height discrimination. The background was determined at both ends of each $\theta/2\theta$ scan. Unit cell dimensions for Ti_3Zn_{22} were determined by least-squares refinements of the best angular positions for 25 independent reflections ($18° < 2\theta < 50°$). The resulting lattice constants agreed rather well with those of the Guinier powder data (Table 1). Empirical absorption corrections were made on the basis of psi-scan data.

Both structures were solved by direct methods with the SHELXS-86 (7) program system and refined by full-matrix least-squares methods of the SDP package (8) with atomic scattering factors (9), corrected for anomalous dispersion (10). Weights were assigned according to the counting statistics and a parameter accounting for isotropic secondary extinction was refined and applied to the calculated structure factors. To check for deviations from the ideal composition, occupancy parameters were refined in one series of least-squares cycles. The resulting occupancies varied between 0.992(2) for Zn7 and 1.001(2) for Zn5 in Ti_3Zn_{22} and between 0.982(5) for Ti and 1.004(2) for Zn3 in $TiZn_{16}$. The only exception was the Ti2 position of Ti_3Zn_{22}, which obtained an occupancy value of 1.082(4). Therefore, in the final least-squares cycles all occupancy parameters were assumed to be ideal with the exception of the Ti2 position of Ti_3Zn_{22}, which was varied with mixed Ti/Zn occupancy resulting in a ratio of 84.1(8)/15.9(8)%. Thus the exact formula of the compound is $Ti_{2.841(8)}Zn_{22.159(8)}$. For Ti_3Zn_{22} (with the corresponding values for $TiZn_{16}$ in parentheses), the refinement resulted in the conventional and weighted residuals of R = 0.020 (0.022) and R_w = 0.020 (0.026) for 64 (50) variable parameters and 920 (787) F values. Final difference Fourier maps showed electron densities of only 1.1 and 0.6 e/Å^3, which were furthermore too close to zinc positions to be suitable for the accommodation of any additional atoms. The atomic parameters are given in Table 2. Listings of the anisotropic thermal parameters and the structure factors are available from the authors.

TABLE 2
Atomic Parameters of Ti_3Zn_{22} and $TiZn_{16}$

Atom		x	y	z	B_{eq}
		$Ti_{2.841(8)}Zn_{22.159(8)}$ ($P4_2/mbc$)			
Ti1	8*h*	0.34415(9)	0.08834(9)	0	0.39(2)
Ti2(15.9% Zn)	4*b*	0	0	¼	0.73(2)
Zn1	16*i*	0.04329(4)	0.23523(4)	0.31747(5)	0.750(8)
Zn2	16*i*	0.05903(4)	0.39714(5)	0.11772(5)	0.902(8)
Zn3	16*i*	0.17348(5)	0.17275(5)	0.15131(6)	1.199(9)
Zn4	16*i*	0.20004(5)	0.06357(5)	0.38435(5)	0.970(9)
Zn5	8*h*	0.10527(7)	0.01180(8)	0	1.15(1)
Zn6	8*h*	0.24115(7)	0.32150(7)	0	0.87(1)
Zn7	8*g*	0.11964(5)	$x + \frac{1}{2}$	¼	0.842(8)
		$TiZn_{16}$ ($Cmcm$)			
Ti	4*c*	0	0.0471(1)	¼	0.52(2)
Zn1	16*h*	0.16810(8)	0.18640(5)	0.07021(4)	1.226(9)
Zn2	16*h*	0.20543(9)	0.44755(5)	0.13535(5)	1.481(9)
Zn3	8*g*	0.33361(1)	0.14449(8)	¼	1.23(1)
Zn4	8*f*	0	0.17634(7)	0.64058(7)	1.42(1)
Zn5	8*f*	0	0.61925(7)	0.03071(7)	1.12(1)
Zn6	4*c*	0	0.2882(1)	¼	1.43(2)
Zn7	4*a*	0	0	0	1.26(2)

Note. The last column contains the equivalent isotropic B values in units of 10^{-2} nm^2. The Ti2 position of Ti_3Zn_{22} was found to have mixed occupancy, which refined to a Ti/Zn ratio of 0.841(8)/0.159(8).

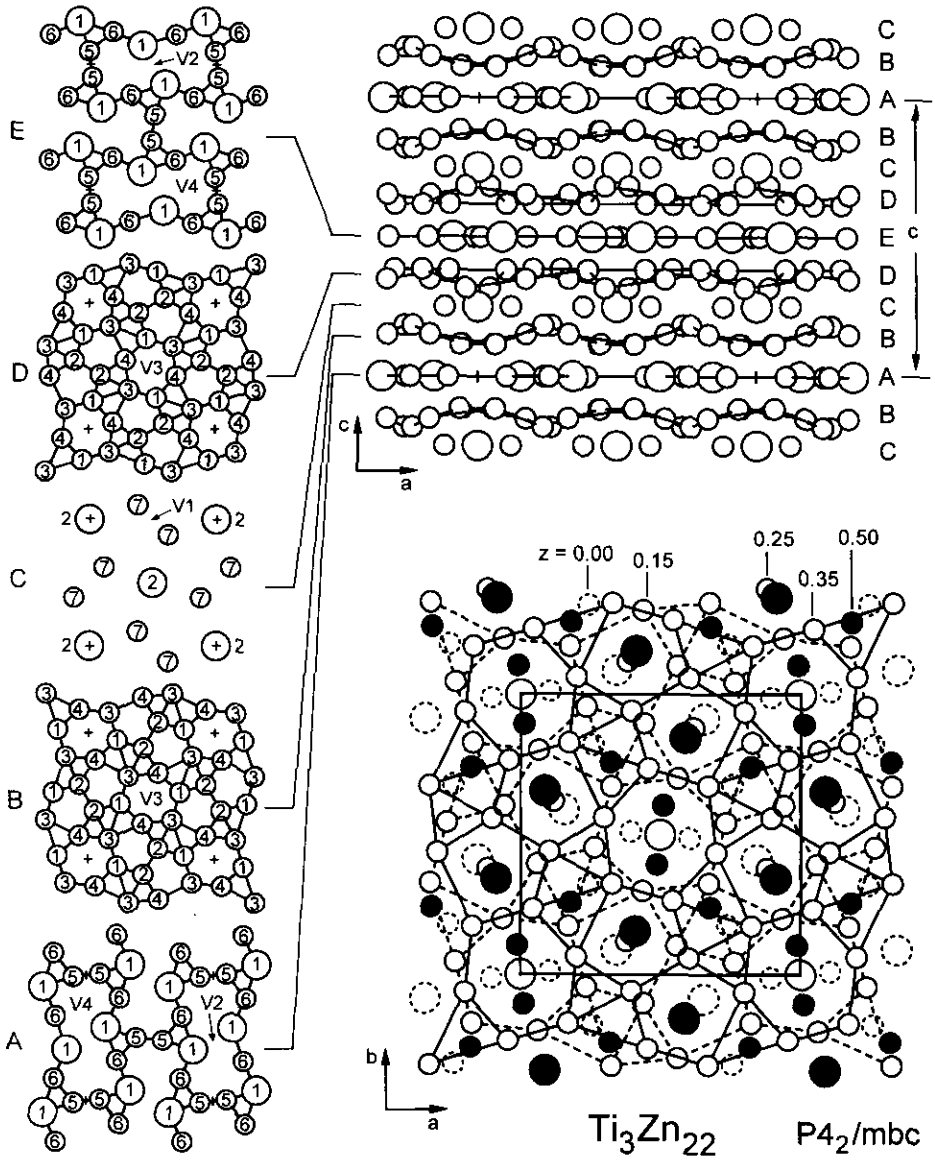

FIG. 3. The crystal structure of Ti_3Zn_{22}: large circles, Ti; small circles, Zn. Single-digit numbers correspond to the atom designations. One-half of the tetragonal cell is projected along the c axis in the plot at the lower right-hand corner. Atoms joined by dashed lines belong to the main layer **B** at $z \approx 0.15$; those joined by solid lines belong to the other main layer **D** with $z \approx 0.35$. Dashed circles and solid black circles represent atoms of the secondary layers **A** and **E** at $z = 0$ and $z = 0.5$. The unconnected atoms (in the centers of the hexagons and pentagons) of layer **C** are at $z = 0.25$. Some positions of the voids V1–V4 are indicated in the layers at the left-hand side.

DISCUSSION

Ti_3Zn_{22} crystallizes with a new structure type. The structure of $TiZn_{16}$ also has a unique crystal structure, which has been determined before (6) from single-crystal data and refined to a residual of $R = 0.11$ for 407 F values. Our structure refinement of the $TiZn_{16}$ structure is considerably more accurate and confirms the earlier work. We have not made a systematic investigation of the zinc-rich portion of the titanium–zinc phase diagram, but we have not observed any indications for an additional phase between $TiZn_3$ and Zn, other than Ti_3Zn_{22} and $TiZn_{16}$.

Both the Ti_3Zn_{22} and the $TiZn_{16}$ structures may be considered as being built up by atomic layers, as is demonstrated in Figs. 3 and 4. The layers designated **B** and **D** in the structure of Ti_3Zn_{22} and the layer **B** of $TiZn_{16}$ consist only of zinc atoms, while the other layers of the two structures contain both atomic species. It can be seen that layers **A** and **E** as well as **B** and **D** of the Ti_3Zn_{22} structure are related by symmetry. The third layer type

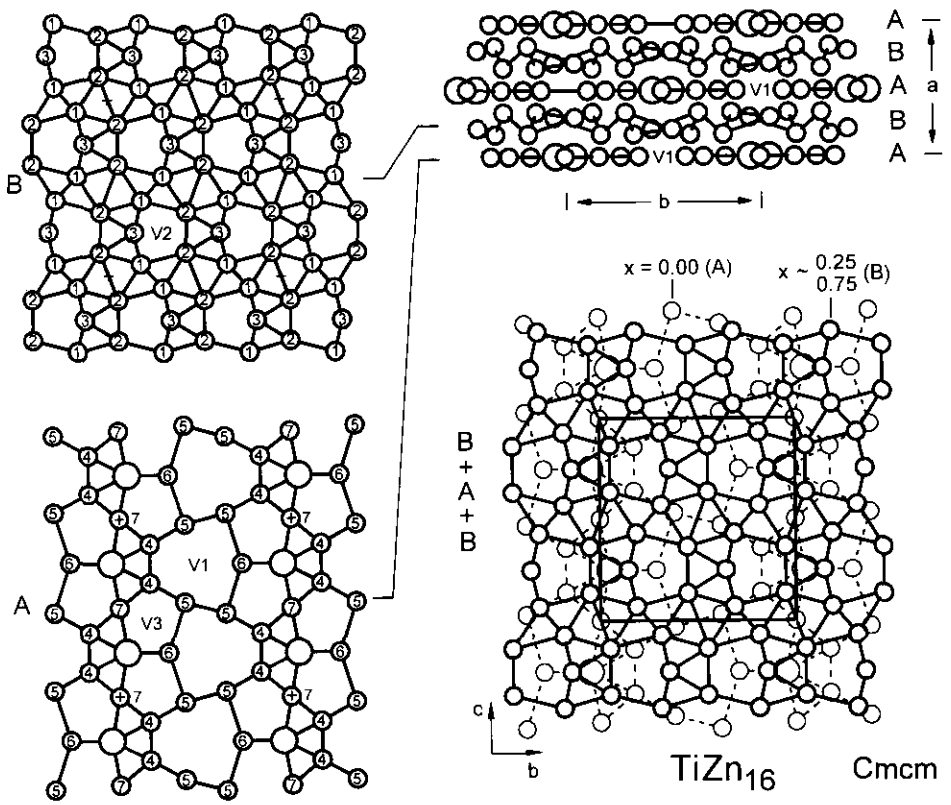

FIG. 4. Crystal structure of $TiZn_{16}$. As can be seen from the projection at the upper right-hand corner, the structure may be considered as a stacking of the two layers **A** and **B**, which are viewed along the *a* axis in the other three projections. Single-digit numbers indicate the atom designations. Some positions of the large unoccupied interstitial sites V1, V2, and V3 are also shown.

C has a low population and the atoms within that layer are not in contact with each other. Only two types of layers are present in the structure of $TiZn_{16}$. Layer **B** of $TiZn_{16}$ and layers **B** and **D** of Ti_3Zn_{22} are puckered, while the others are flat.

The coordination polyhedra of both structures are shown in Fig. 5. The corresponding interatomic distances are listed in Table 3. The only exception concerns the Zn5–Zn6 distance of 347.7 pm in $TiZn_{16}$. The corresponding atoms were not shown in the coordination polyhedra of these zinc atoms.

In both structures the titanium atoms have only zinc atoms in their coordination sphere. The Ti1 atoms of Ti_3Zn_{22} have 15 zinc neighbors covering the range from 279.6 to 322.8 pm with an average of 289.7 pm. This distance is practically the same as the average Ti–Zn distance of 289.1 pm for the titanium atom in $TiZn_{16}$, which also has 15 zinc neighbors. The Ti2 atoms of Ti_3Zn_{22} have the higher coordination number 16 and consequently their average Ti–Zn distance is somewhat longer with 297.0 pm.

The zinc atoms have coordination numbers varying between 11 (Zn6 in Ti_3Zn_{22}, Zn3 and Zn6 in $TiZn_{16}$) and 14 (Zn3 in Ti_3Zn_{22}). Only the Zn5 atom of $TiZn_{16}$ has no titanium neighbor. In that compound all of the other zinc atoms have one titanium neighbor with the exception of the Zn7 atom, which has two. In agreement with the higher titanium content of Ti_3Zn_{22}, most zinc atoms have two titanium neighbors in that compound. The only exception is the Zn5 atom, which has three titanium neighbors. This coordination polyhedron is also remarkable, because it has an exceptionally short Zn5–Zn5 distance of 244.1 pm. All other Zn–Zn distances are greater than 252 pm. An almost equally short Zn–Zn distance was found in $NbZn_2$ with 245 pm (11).

Generally it is found that intermetallic compounds have close packed structures with high coordination numbers for all atoms. Therefore it is remarkable that the structures of Ti_3Zn_{22} and $TiZn_{16}$ contain relatively large voids. In Figs. 3 and 4 we have labeled the largest voids of both structures with the symbols V1–V4. Their positions and the distances from the approximate centers of these voids to the neighboring atomic sites are listed in Table 4. These are only the largest voids. Smaller ones are also present; e.g., a void V5 in Ti_3Zn_{22} (close to V4 at $x = 0.871$, $y = 0.205$, $z = 0$, not shown in Fig. 3) has two zinc atoms as

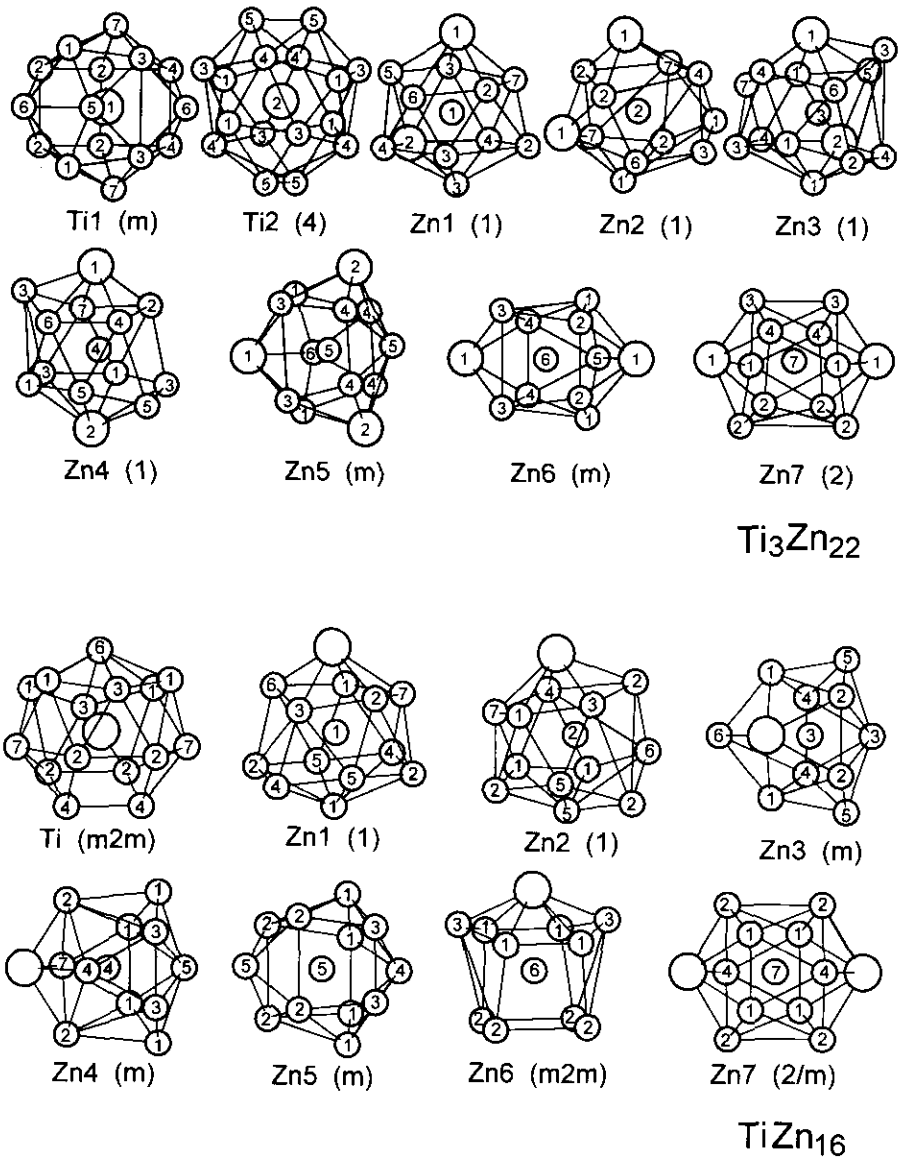

FIG. 5. Coordination polyhedra in the structures of Ti_3Zn_{22} and $TiZn_{16}$: large circles, Ti; small circles, Zn. The numbers correspond to the atom designations. The site symmetries of the central atoms are indicated in parentheses.

nearest neighbors at 153 pm, and the void V3 of $TiZn_{16}$ shown in Fig. 4 has two close zinc neighbors at 130 pm. They are certainly unsuited for the accommodation of additional atoms, unless the positional parameters of the host structures are changed.

This is not necessarily the case for the voids V1–V4 of Ti_3Zn_{22} nor for the voids V1 and V2 of $TiZn_{16}$. These voids are large enough to accommodate small atoms like carbon, nitrogen, or oxygen. In the NaCl-type structure of the vanadium carbide VC (12), the carbon atoms occupy octahedral voids with V–C distances of 208 pm. Since vanadium and zinc have similar atomic radii in intermetallic compounds (for the coordination number 12) (13), this distance can be directly compared with the distances listed in Table 4, and it can be seen that several of these voids are large enough to accommodate interstitial atoms. Our structure refinements showed no significant electron densities at any of these sites. However, these sites could be occupied in ternary compounds not yet synthesized, e.g., $Ti_3Mn_{22}C_{6-x}$ or $TiMn_{16}C_{3-x}$. Similar correspondences have been noted before. For instance $Pr_2Mn_{17}C_{3-x}$ crystallizes with a structure in which the carbon atoms occupy interstitial voids of the Th_2Zn_{17}-type structure (14). Other examples were enumerated recently (15). The

TABLE 3
Interatomic Distances in Ti_3Zn_{22} and $TiZn_{16}$

Ti_3Zn_{22}

Ti1:	2Zn3	279.6	Zn2:	1Ti1	281.4	Zn4:	1Ti2	286.7	Zn6:	1Ti1	293.7
	2Zn2	281.4		1Ti1	282.5		1Ti1	297.2		1Ti1	322.8
	2Zn2	282.5		1Zn7	256.4		1Zn6	262.3		2Zn3	255.9
	2Zn1	287.2		1Zn1	257.7		1Zn1	265.0		2Zn1	262.2
	1Zn5	289.1		1Zn6	264.2		1Zn4	265.1		2Zn4	262.3
	2Zn7	291.7		1Zn4	267.5		1Zn7	266.5		2Zn2	264.2
	1Zn6	293.7		1Zn2	269.7		1Zn2	267.5		1Zn5	281.8
	2Zn4	297.2		1Zn2	273.3		1Zn3	278.0	Zn7:	2Ti1	291.7
	1Zn6	322.8		1Zn3	292.8		1Zn1	278.6		2Zn2	256.4
Ti2:	4Zn1	286.2		1Zn1	295.8		1Zn5	281.9		2Zn1	263.0
	4Zn4	286.7		1Zn7	305.9		1Zn3	296.7		2Zn4	266.5
	4Zn3	303.9		1Zn2	311.4		1Zn5	320.1		2Zn3	270.8
	4Zn5	311.3	Zn3:	1Ti1	279.6		1Zn3	339.1		2Zn2	305.9
Zn1:	1Ti2	286.2		1Ti2	303.9	Zn5:	1Ti1	289.1			
	1Ti1	287.2		1Zn1	252.8		2Ti2	311.3			
	1Zn3	252.8		1Zn6	255.9		1Zn5	244.1			
	1Zn2	257.7		1Zn1	261.4		2Zn1	264.9			
	1Zn3	261.4		1Zn5	265.8		2Zn3	265.8			
	1Zn6	262.2		1Zn7	270.8		1Zn6	281.8			
	1Zn7	263.0		1Zn4	278.0		2Zn4	281.9			
	1Zn4	264.9		1Zn2	292.8		2Zn4	320.1			
	1Zn5	265.1		1Zn4	296.7						
	1Zn4	278.6		1Zn3	337.5						
	1Zn2	295.8		1Zn4	339.1						
	1Zn3	345.6		1Zn1	345.6						
				1Zn3	346.7						

$TiZn_{16}$

Ti:	1Zn6	275.2	Zn2:	1Ti	287.5	Zn3:	1Ti	279.9	Zn5:	2Zn2	263.1
	2Zn3	279.9		1Zn5	263.1		2Zn1	252.1		1Zn4	266.9
	2Zn4	285.9		1Zn3	264.1		1Zn3	256.2		2Zn1	270.8
	4Zn2	287.5		1Zn4	267.3		2Zn2	264.1		2Zn2	280.5
	4Zn1	295.0		1Zn2	270.6		2Zn4	273.7		1Zn5	281.7
	2Zn7	299.9		1Zn6	276.4		2Zn5	290.2		2Zn1	283.1
Zn1:	1Ti	295.0		1Zn5	280.5		1Zn6	304.8		2Zn3	290.2
	1Zn3	252.1		1Zn7	283.8	Zn4:	1Ti	285.9		(1Zn6	347.7)
	1Zn1	253.9		1Zn1	299.5		1Zn4	258.2	Zn6:	1Ti	275.2
	1Zn1	258.8		1Zn1	302.8		1Zn7	260.8		4Zn1	274.4
	1Zn7	262.5		1Zn1	309.2		1Zn5	266.9		4Zn2	276.4
	1Zn5	270.8		1Zn2	316.3		2Zn2	267.3		2Zn3	304.8
	1Zn6	274.4		1Zn2	341.1		2Zn3	273.7		(2Zn5	347.7)
	1Zn4	280.6					2Zn1	280.6	Zn7:	2Ti	299.9
	1Zn5	283.1					2Zn1	311.0		2Zn4	260.8
	1Zn2	299.5								4Zn1	262.5
	1Zn2	302.8								4Zn2	283.8
	1Zn2	309.2									
	1Zn4	311.0									

Note. All distances shorter than 370 pm are given. All standard deviations are 0.2 pm or less.

TABLE 4
Location and Coordination of Unoccupied Sites □ (voids V) in the Structures of Ti_3Zn_{22} and $TiZn_{16}$

		x	y	z
		$Ti_3Zn_{22}\square_6$		
V1	4*d*	0	½	¼
V2	4*c*	0	½	0
V3[a]	16*i*	0.055	0.006	0.102
V4	8*h*	0.074	0.243	0
		$TiZn_{16}\square_3$		
V1	4*c*	0	0.495	¼
V2	8*g*	0.235	0.320	¼

	$Ti_3Zn_{22}\square_6$			$TiZn_{16}\square_3$	
V1:	2Zn7	195 pm	V1:	2Zn3	213 pm
	4Zn2	204		4Zn2	215
V2:	2Ti1	206		1Zn6	236
	4Zn2	192		2Zn5	295
V3:	1Ti2	181	V2:	1Zn3	205
	1Zn5	180		2Zn2	206
	1Zn4	181		1Zn6	215
	1Zn5	181		2Zn4	216
	1Zn3	254		2Zn1	274
	1Zn1	280			
V4:	2Zn4	212			
	1Zn6	213			
	2Zn3	223			
	2Zn2	224			
	1Zn5	269			

[a] The voids V3 of Ti_3Zn_{22} are very close to each other; thus, only half of them could be occupied in a hypothetical "filled" Ti_3Zn_{22} structure.

voids in the structures of Ti_3Zn_{22} and $TiZn_{16}$ might accommodate nonbonding electrons, as was discussed for the structure of Ni_3Sn_4 (16).

Even though the structures of Ti_3Zn_{22} and $TiZn_{16}$ contain large voids, the average atomic volumes of these two compounds do not deviate greatly from the smooth plot of the average volume/atom curve of the binary system titanium–zinc (Fig. 6). The structures of the other compounds of this system with high zinc content probably have similar locations with low packing efficiency. We have not investigated this, however, this is well known for elemental zinc. It has a hexagonal "close-packed" structure with the unusually high c/a ratio of 1.856, considerably different from the ideal ratio of 1.63. As a consequence the zinc atoms in the elemental structure have six

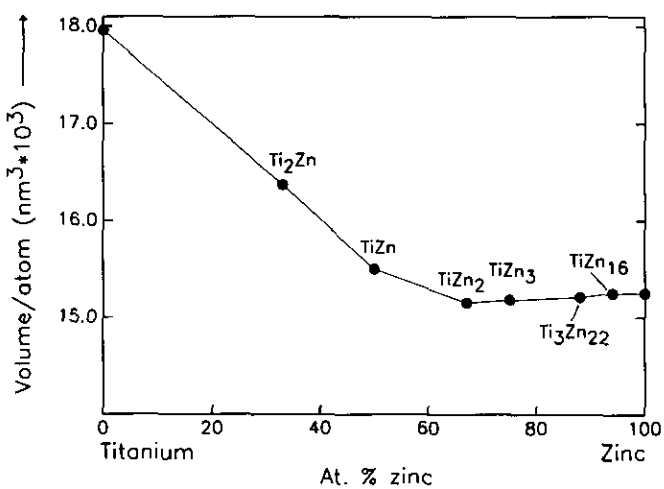

FIG. 6. Average atomic volume in the binary system titanium–zinc.

close neighbors at 264.4 pm, while the other six neighbors are at the considerably larger distance of 291.2 pm (17).

It is difficult to calculate the band structures and to discuss the chemical bonding of Ti_3Zn_{22} and $TiZn_{16}$ because there are too many atoms in their unit cells. But we can visualize the electronic structures on the basis of that of $ZrZn_2$ (18). Zn has a lower atomic orbital energy relative to Ti, and as a result, the band complex derived from the Zn 3*d* orbitals would be at the lower energy below the Fermi energy E_f and completely filled. The character of the bands near E_f might be determined mainly by the Ti 3*d* orbitals with smaller contributions from the *p* states of both the Ti and Zn atoms, indicating the Ti–Zn covalent bonding interactions. The Fermi level would be crossed by 24 Ti 3*d*-like dispersive bands for Ti_3Zn_{22} and by 4 Ti 3*d*-like bands for $TiZn_{16}$, which are characteristic of metallic-type materials, consistent with the electrical conductivity and magnetic susceptibility measurements.

ACKNOWLEDGMENTS

We thank Dipl. Ing. U. Rodewald and Dr. M. H. Möller for the collection of the single-crystal intensity data and Dr. R.-D. Hoffmann for the help in solving the crystal structure. We appreciate a generous gift of silica tubes by Dr. G. Höfer of the Heraeus Quarzschmelze. We also thank the Alexander von Humboldt Foundation for a stipend to Xue-an Chen. This work was supported by the Deutsche Forschungs gemeinschaft and the Fonds der Chemischen Industrie.

REFERENCES

1. W. Heine and U. Zwicker, *Z. Metallkd.* **53,** 380 (1962).
2. W. Rossteutscher and K. Schubert, *Z. Metallkd.* **56,** 730 (1965).
3. E. H. Rennhack, *Trans. Metall. Soc. AIME* **236,** 941 (1966).
4. P. Pietrokowsky, *Trans. Metall. Soc. AIME* **200,** 219 (1954).
5. G. L. Leone and H. W. Kerr, *J. Cryst. Growth* **32,** 111 (1976).
6. M. Saillard, G. Develey, C. Becle, J. M. Moreau, and D. Paccard, *Acta Crystallogr. Sect. B* **37,** 224 (1981).
7. G. M. Sheldrick, SHELXS-86, a computer program for crystal structure determination, Univ. Göttingen, Germany, 1986.
8. B. A. Frenz & Associates, Inc. and Enraf Nonius, 1986.
9. D. T. Cromer and J. B. Mann, *Acta Crystallogr. Sect. A: Found. Crystallogr.* **24,** 321 (1968).
10. D. T. Cromer and D. Liberman, *J. Chem. Phys.* **53,** 1891 (1970).
11. C. L. Vold, *Acta Crystallogr.* **14,** 1289 (1961).
12. P. Villars and L. D. Calvert, "Pearson's Handbook of Crystallographic Data for Intermetallic Phases." The Materials Information Society, Materials Park, OH, 1991.
13. E. Teatum, K. Gschneidner, Jr., and J. Waber, LA-2345, U. S. Department of Commerce, Washington, DC, 1960.
14. G. Block and W. Jeitschko, *Inorg. Chem.* **25,** 279 (1986).
15. W. Jeitschko, G. Block, G. E. Kahnert, and R. K. Behrens, *J. Solid State Chem.* **89,** 191 (1990).
16. W. Jeitschko and B. Jaberg, *Acta Crystallogr. Sect. B* **38,** 598 (1982).
17. J. Donohue, "The Structures of the Elements." Wiley, New York, 1974.
18. M.-C. Huang, H. J. F. Jansen, and A. J. Freeman, *Phys. Rev. B: Condens. Matter* **37,** 3489 (1988).